Direct Observation of the Effect of Solute on Complex HSLA Steel Microstructures

Michael Grimes[1], Matthew Hartshorne[2], Christopher Winkler[2], Pello Uranga[3], Mitra L. Taheri[2]

[1]Lehigh University, Department of Materials Science and Engineering, Bethlehem. PA
[2]Drexel University, Department of Materials Science and Engineering, Philadelphia, PA
[3] CEIT and TECNUN, University of Navarra, San Sebastian, Spain

Introduction

HSLA (high strength low alloy) steels are used in various applications, from building frames to oil and gas pipelines:

Figure 1: Alaskan Pipeline

Figure 2: HSLA Steel Pipes

Figure 3: HSLA Steel Building Frame

This is due to their high strength and toughness at a wide range of temperatures [1]. Vanadium (V) and Molybdenum (Mo) are added to Niobium (Nb) based HSLA steels to increase strength and toughness by (1) suppressing pearlite formation and increasing acicular ferrite content [2] and (2) slowing the diffusion of the carbide forming species delaying precipitate nucleation and growth [3].

There is little understanding of critical interactions between the many different alloying elements during transformations. The goal of this project is to understand the difference in the formation, growth, migration and interactions of precipitates, dislocations, and grain boundaries in Nb-V and Nb-Mo HSLA steels (Tables 1 and 2). These changes were studied during three different heat treatments (Figure 4) using a multiscale *ex situ* and *in situ* electron microscopy approach.

Compositions and Processing

Nb-V Steel

C	Mn	Si	P	S	Al	Nb	V	N
0.06	1.12	0.29	0.02	0.007	0.035	0.062	0.053	0.0081

Table 1: Alloy composition of Nb-V HSLA steels

Nb-Mo Steel

C	Mn	Si	P	S	Al	Nb	Mo	N
0.047	1.6	0.054	0.011	0.002	0.03	0.061	0.16	0.005

Table 2: Alloy composition of Nb-Mo HSLA steels

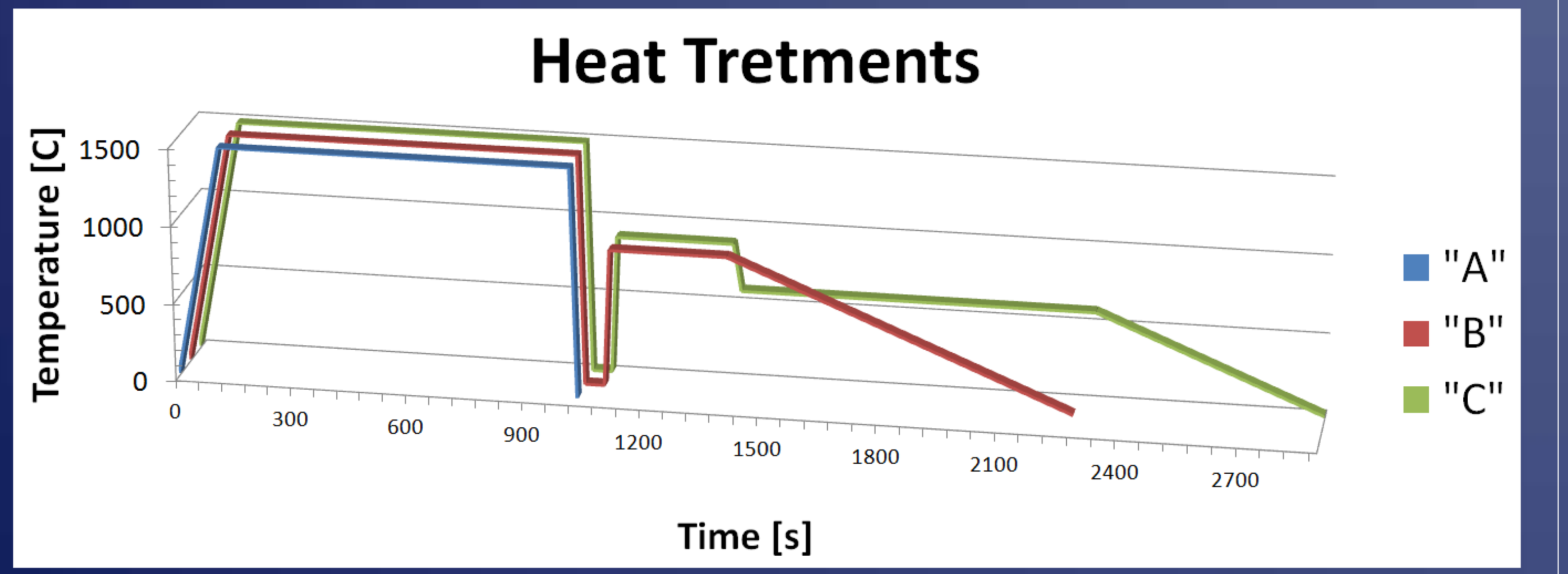

Figure 4: Time temperature graph for the three heat treatments

Methods

In this project, *in situ* and *ex situ* methods were used to study the difference in microstructureal evolution of the two HSLA steel alloys.

- Light Optical Microscopy – Basic microstructure
- Scanning Electron Microscopy – Fine microstructures
- Electron Backscatter Diffraction – Preferential grain orientation
- Transmission Electron Microscopy – *Ex situ* and *in situ*

Data/Results

Primary microstructures varied by temper, while alloying composition effected secondary microstructures.

- "A" heat treat→ predominantly martinsitic lath structure.
- "B" heat treat→ predominantly equiaxed ferritic grains.
- "C" heat treat→ predominantly smaller ferritic grains.

Acicular ferrite (AF) is present in the Nb-Mo samples while pearlite is seen in the Nb-V sample (Figures 6 and 7). Mo does a good job suppressing pearlite formation and increasing AF formation. Both microstructures limit crack propagation, but AF is stable at higher temperatures. Thus, Nb-Mo steels are stronger at higher temperatures.

The grains in the "C" heat treated samples were smaller and more irregular than in the "B" heat treated samples. Precipitate pinning and subgrain formation were observed during "B" *in situ* tempering of the Nb-V steel. Precipitate formation at ~475°C and dissolution at ~800°C were observed, showing that some precipitates are stable during tempering at 600°C, but not at 900°C. We attribute the smaller grain sizes in the "C" samples to these findings.

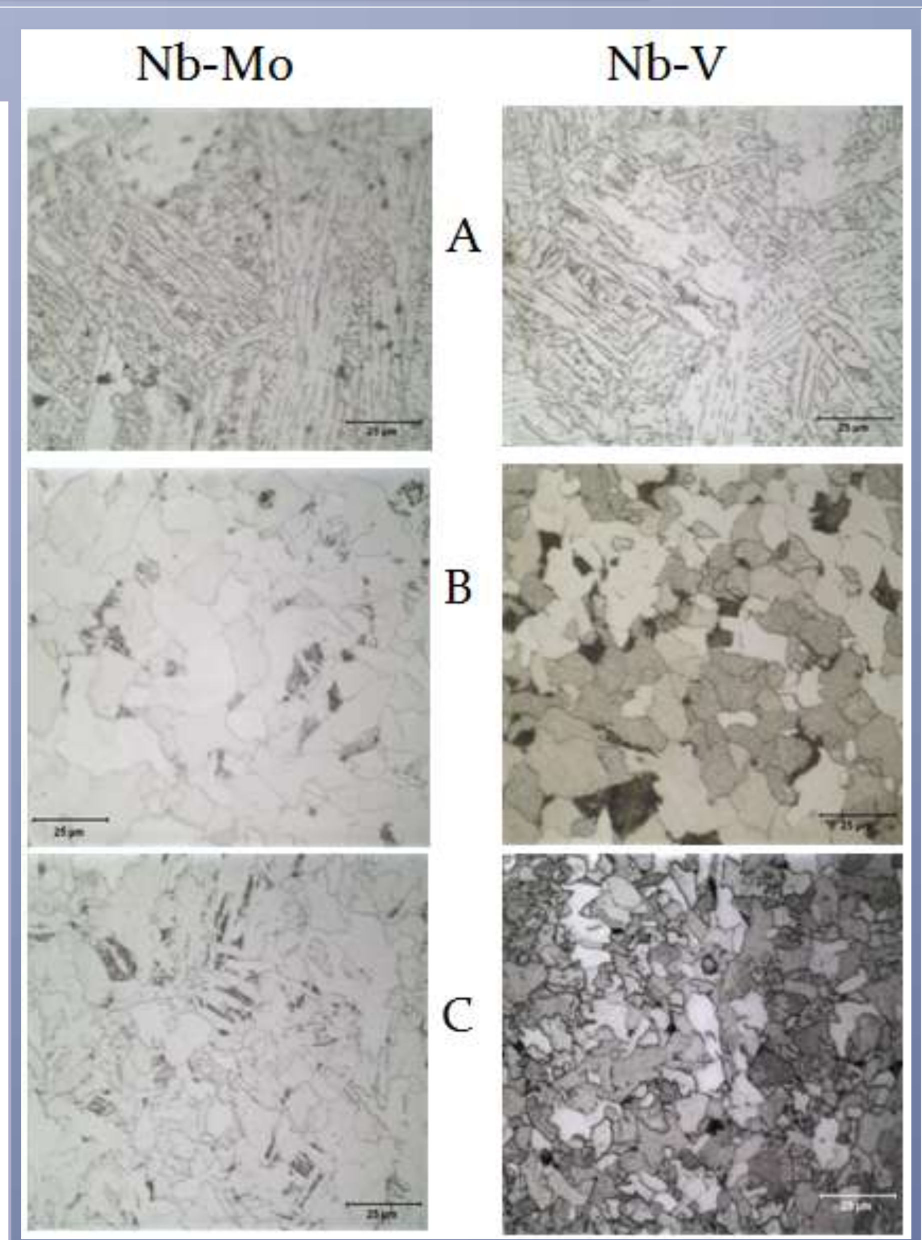

Figure 5: LOM pictures of all six samples

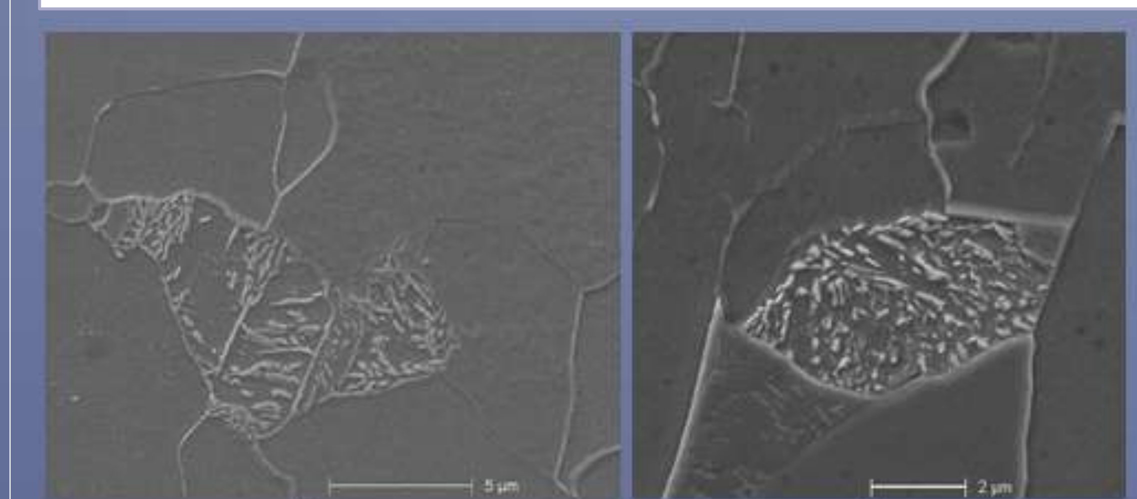

(a) (b)

Figure 6: Acicular ferrite structure in Mb-V HSLA steel with B and C heat treatment in (a) and (b) respectively

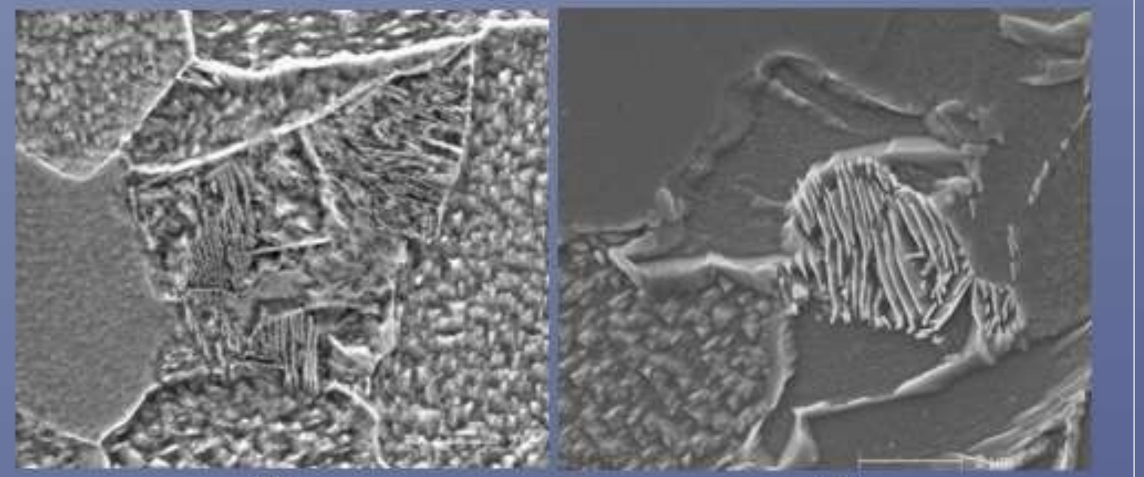

(a) (b)

Figure 7: Pearlite microstructure in Nb-V HSLA steel with B and C heat treatment in (a) and (b) respectively

Nb-Mo and the Nb-V steels exhibited different dislocation networks. The Nb-Mo sample contained dislocation loops (Figure 8). In the Nb-V samples dislocation pile ups and dislocations-precipitate interactions were revealed during tempering (Figures 9-11). After the dislocations annihilated, strings of precipitates can be observed (Figure 10).

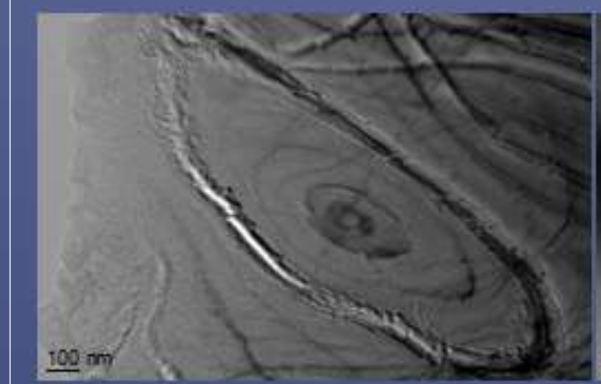

Figure 8: Dislocation loop in the "B" heat treated Nb-Mo sample

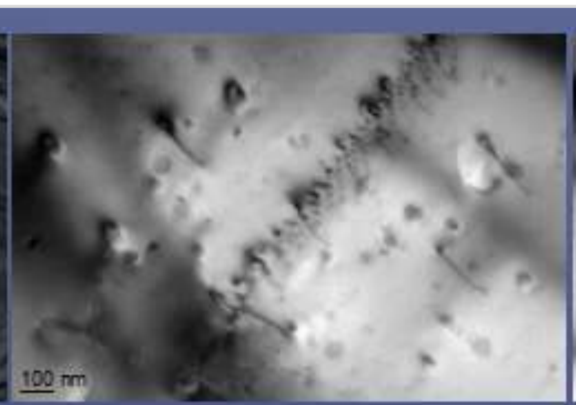

Figure 9: Dislocation pile up that dragged precipitates in the "B" *in situ* heat treated Nb-V sample

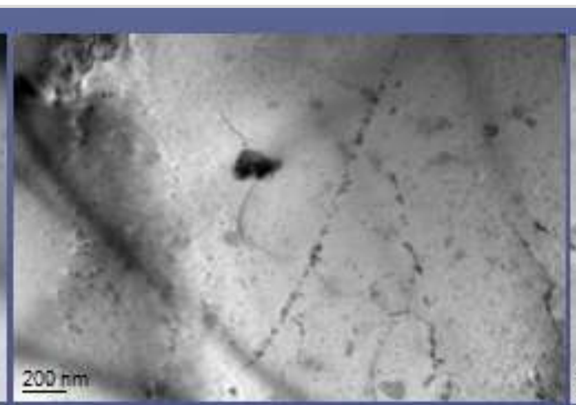

Figure 10: String of precipitates in the "B" heat treated Nb-V sample

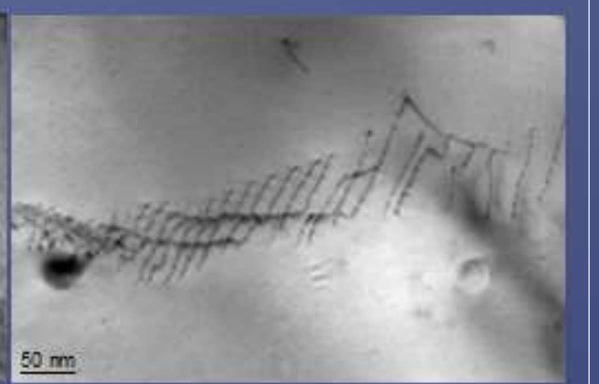

Figure 11: Dislocation pile up in the "C" heat treated Nb-V sample

EBSD maps reveal no preferred grain orientation from "B" to "C" heat treat (Figure 12), however the grains become more elongated in the Nb-Mo steels during the "C" heat treat (Figure 12b).

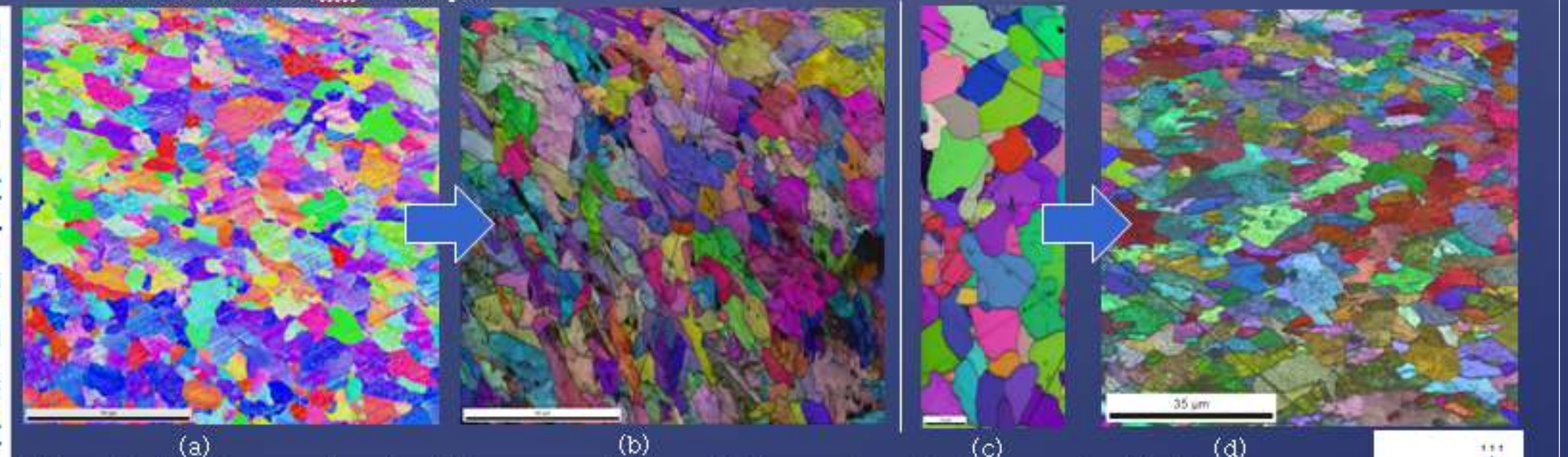

Figure 12: EBSD scans showing (a) inverse pole figure (IPF) maps from Nb-Mo sample with "B" heat treatment (b) IPF map from Nb-Mo sample with "C" heat treatment, (c) IPF map of Nb-V sample with "B" heat treatment, (d) IPF map of Nb-V sample with "C" heat treatment, along with (e) a key to showing grain orientation

Conclusion

1. Precipitate pinning during tempering at 600°C caused a decrease in grain size in the "C" heat treated samples.
2. Mo is better than V at suppressing pearlite formation when coupled with Nb in HSLA steels.
3. Dislocations became tangled with precipitates, causing the dislocations to drag the precipitates into lines during tempering. This effect was more common in the Nb-V alloys.
4. Dislocation networks found in the Nb-Mo samples were primarily loops, while the Nb-V samples contained dislocation pile-ups.
5. Overall dislocation density was higher in the Nb-Mo samples.
6. No preferential grain orientation existed in either alloy, however the Nb-Mo "C" heated sample had elongated grains.

Future Work

- Additional *ex situ* TEM imaging on the Nb-Mo alloy after the "C" heat treat.
- Complete *in situ* tempering on the Nb-Mo alloy.
- Further in situ tempering of the Nb-V alloy:
  - → During "B" heat treat, connect dislocation formation and first precipitate intersection.
  - → During the "C" heat treat, look for why the dislocation pile ups are not associated with precipitates as much as was seen in the "B" heat treated alloys.

References

[1]W.B. Lee, S.G. Hong, C.G. Park, K.H. Kim and S.H. Park, *Scripta Mater.* **43** (2000), p.319.
[2]Y. Li, D.N. Crowther, M.J.W. Green, P.S. Mitchell, and T.N. Baker, *ISIJ Int.* **41** (2001) p.46.
[3]M.G. Akben, B. Barcoix, J.J. Jonas, *Acta Metall.* **31** (1983), p.161.

Acknowledgements

The authors acknowledge the use of the Centralized Research Facility (CRF) in the College of Engineering at Drexel University as well as Dr. Edward Basgall and Dr. Craig Johnson.

The National Science Foundation under Grant No. EEC 0649033 [DREAM]